Electron capture in N^{2+}-He and N^{2+}-Ne collisions

Yukinori Sato* and John H. Moore
Chemistry Department, University of Maryland, College Park, Maryland 20742
(Received 15 June 1978)

The kinetic-energy change in electron-capture collisions between N^{2+} and He or Ne in the collision energy range 0.2–2.4 keV has been observed with sufficient resolution to separate all possible final states. These processes were modeled in terms of both a curve-crossing and a noncrossing mechanism. The results suggest that the observed transitions occur at an intermediate internuclear separation, $(3.5–8)a_0$, and that the noncrossing mechanism is important when an appropriate crossing does not occur within this range.

I. INTRODUCTION

Electron capture in ion-atom collisions,

$$A^{n+}+B \rightarrow A^{(n-1)+}+B^{+}$$

has long been recognized as a typical example of a reaction which proceeds through a curve-crossing mechanism.[1,2] In this model of the process the transition from initial to final state is supposed to occur near the crossing point of a pair of molecular potential energy curves which correspond to different separated atom states. Early investigations by Landau,[3] Zener,[4] and Stueckelberg[5] resulted in the well known Landau-Zener (LZ) formalism to describe this process. More recently, however, detailed quantum-mechanical calculations have brought into question the range of applicability of the LZ formula.[6]

A number of experimental studies of electron capture by multiply charged ions have been made. Hasted and his colleagues measured the total cross sections for single-electron capture by N^{2+}, C^{2+}, Ar^{2+}, and Kr^{m+} in collisions with rare-gas atoms.[7] These data were analyzed in terms of the LZ formalism to deduce the magnitude of the coupling matrix elements at curve-crossing points which were assumed to be important in the observed processes.[2,7,8] More recently they measured angular differential cross sections for electron capture by C^{2+}, N^{2+}, and O^{2+} on He and Ne.[9,10] Chen and co-workers have measured cross sections differential in angle and energy for He^{2+} on He at kinetic energies from 200 to 600 eV.[11] All of these studies have been made with sufficient angular resolution to observe the characteristic structure in the differential cross section as a function of angle, however, the energy resolution has not been sufficient to determine uniquely the final state of the system.

For an electron-capture process which is only slightly exothermic, the curve crossing may occur at a large internuclear separation where the coupling between initial and final states is very small. In this event the probability of a transition occurring at small internuclear distances may be large compared to that for a transition at the crossing point. A useful model for this process, known as the "Demkov mechanism,"[12] predicts that a transition is likely to occur at an internuclear distance where the coupling between initial and final states is comparable to the separation between the corresponding potential energy curves. The Demkov mechanism has been successfully applied in the elucidation of asymmetric, near-resonant charge transfer.[13–16]

We report herein a study of the reactions

$$N^{2+}+X \rightarrow N^{+}+X^{+};\quad X=\text{He or Ne}$$

at collision energies of 200–2400 eV. The wide range of final states accessible to these collision systems present a broad sampling of curve-crossing distances and energy defects for the electron-transfer process. The kinetic-energy change of the nitrogen projectile has been measured with sufficient resolution to separate all final states. The collision energy dependence of the cross sections for the processes observed will be discussed in terms of both the curve-crossing and Demkov mechanisms. It will be shown that some of the processes observed are best described in terms of the Demkov mechanism.

II. EXPERIMENTAL

The same apparatus is used for these experiments as was used previously for energy-loss measurements of inelastically scattered, singly charged ions[17] although the lens biasing arrangement has been changed to account for the change in charge state of the ion in the scattering process now under investigation. A beam of N^{2+} at about 8-keV kinetic is produced by a duoplasmatron ion source followed by an extraction lens and a Wien filter. As shown in Fig. 1, this beam is injected

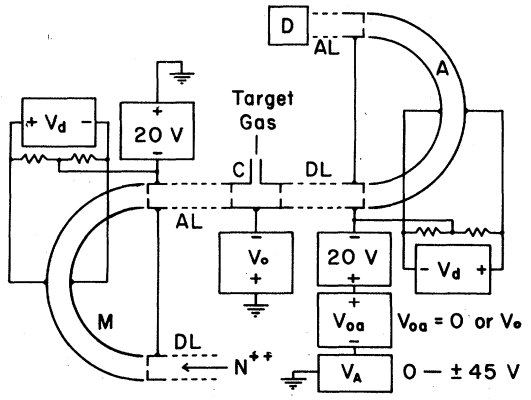

FIG. 1. Schematic diagram of the apparatus showing decelerating (DL) and accelerating (AL) lens systems, the hemispherical electrostatic monochromator (M) and analyzer (A), the collision chamber (C), and the detector (D). Important features of the lens biasing system are illustrated.

into the scattering apparatus which consists of an electrostatic monochromator (M) followed by a target cell and analyzer (A). The bias voltages on important electrodes are also indicated in this figure.

The ion source is at ground potential so that N^{2+} enters the monochromator at 40 eV. Ions with energies within the bandpass of the monochromator are accelerated to the collision cell where they pass through the target gas with a kinetic energy $E_0 = 2eV_0$. Collision energies of 200–2400 eV were employed in these experiments. When V_A and V_{0a} are set to zero, unscattered N^{2+} ions are transmitted to the detector. When $V_A = 0$ and $V_{0a} = V_0$, ions whose charge has changed from 2 to 1, but whose kinetic energy is unchanged are transmitted to the detector. Finally, the change of kinetic energy of ions which have captured an electron can be determined by setting $V_{0a} = V_0$ and scanning V_A thus subtracting or adding energy to permit these ions to be transmitted through the analyzer. The energy gain of N^+ arriving at the detector is $\Delta E = eV_A$, the energy defect of the corresponding electron-capture process. The energy resolution is sufficient to completely resolve all single-electron capture processes from one another.

Most measurements were made at a scattering angle of 0° with a resolution of 1.2° FWHM. This resolution is not sufficient to resolve the oscillatory structure in the differential cross sections.[9,10] In fact, an investigation of the angular distribution of scattered N^+ demonstrated that more than 90% of the scattered ions fell within the field of view of the analyzer when it was positioned at 0° and thus the intensity of a peak in the energy change spectrum of N^+ ions is approximately proportional to the integrated cross section of the corresponding process.

III. RESULTS

The single-electron capture processes which were observed, and the corresponding energy defects are

$$N^{2+}(^2P) + He(^1S) \rightarrow N^+(^3P) + He^+(^2S); \quad \Delta E_1 = 5.02 \text{ eV}, \tag{1a}$$

$$\rightarrow N^+(^1D) + He^+(^2S); \quad \Delta E_2 = 3.12 \text{ eV}, \tag{1b}$$

$$\rightarrow N^+(^1S) + He^+(^2S); \quad \Delta E_3 = 0.97 \text{ eV}; \tag{1c}$$

and

$$N^{2+}(^2P) + Ne(^1S) \rightarrow N^+(^3P) + Ne^+(^2P); \quad \Delta E_1 = 8.05 \text{ eV}, \tag{2a}$$

$$\rightarrow N^+(^1D) + Ne^+(^2P); \quad \Delta E_2 = 6.15 \text{ eV}, \tag{2b}$$

$$\rightarrow N^+(^1S) + Ne^+(^2P); \quad \Delta E_3 = 4.00 \text{ eV}. \tag{2c}$$

As expected from the Wigner spin-conservation rule,[18] charge transfer to give $N^+(^5S)$ was not observed although such a process would have a small energy defect for these collision systems. In the N^{2+}-Ne system, charge transfer to give $N^+(^3D)$ might be expected since this process has a small energy defect, however, it was not observed.[19] Furthermore, electron capture leading to excited He^+ or Ne^+ was not an important process. Only the exoergic processes (1a)–(2c) occurred with any appreciable probability.

The energy change spectra of N^+ from the N^{2+}-He and N^{2+}-Ne collision systems are compared in Fig. 2. The final-state distributions for these two systems are quite different. $N^+(^3P)$ is the major product for the He target while $N^+(^1D)$ is the major product for the Ne target. $N^+(^1S)$ is produced in N^{2+}-Ne collisions but is barely observable for N^{2+}-He collisions.

The variation of the N^+ energy-change spectra as a function of collision energy for the N^{2+}-He and N^{2+}-Ne systems are illustrated in Figs. 3 and 4, respectively. The most striking difference between these two studies is that the cross-section ratio $Q(^3P)/Q(^1D)$ decreases with increasing energy for the N^{2+}-He system and increases with energy for the N^{2+}-Ne system. For the N^{2+}-Ne system the ratio $Q(^1S)/Q(^1D)$ decreases with increasing collision energy.

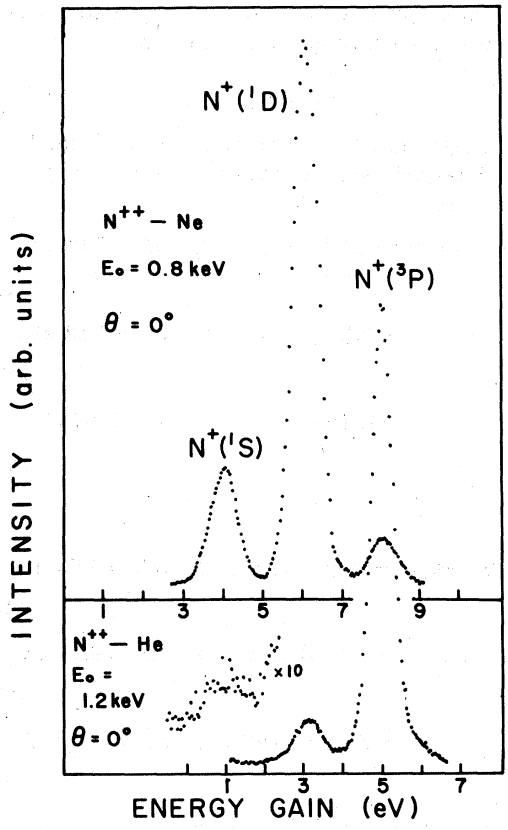

FIG. 2. Representative energy-change spectra of the forward-scattered N^+ produced in electron-capture collisions of N^{2+} with Ne and He.

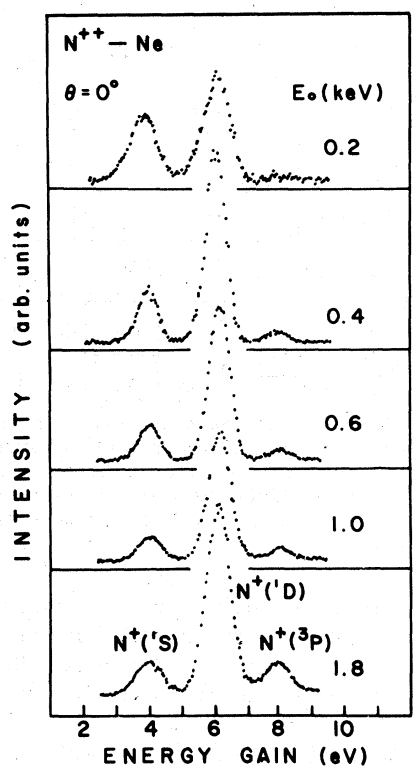

FIG. 4. Energy-change spectra of N^+ produced in electron-capture collisions of 0.2–1.8 keV N^{2+} with Ne.

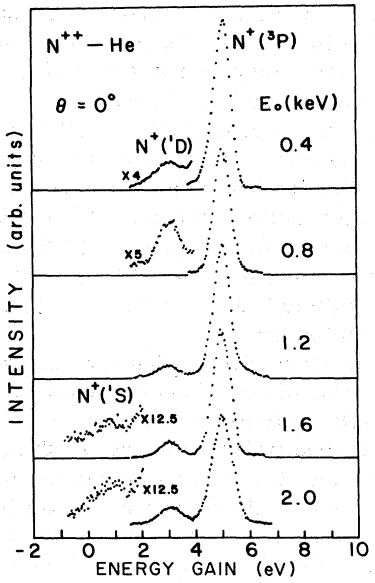

FIG. 3. Energy-change spectra of N^+ produced in electron-capture collisions of 0.4–2.0 keV N^{2+} with He.

IV. DISCUSSION

A. Curve-crossing mechanism

The curve crossings which may be responsible for the processes of interest here are located at relatively large internuclear separations. In this event the diabatic curve representing the initial state can be taken as that corresponding to a charge-induced dipole interaction:

$$V_0(R) = 2\alpha(A)/R^4; \quad A = \text{He or Ne} \tag{3}$$

where R is the distance separating the collision partners and $\alpha(A)$ is the polarizability of the target. The potential energy of the final states arises from the Coulombic interaction and the mutual charge-induced dipole interaction between the final-state ions, in addition the potential energy of the final state relative to the initial state must asymptotically approach the energy defect for the charge-exchange process:

$$V_i(R) = \frac{1}{R} - \frac{1}{2R^4}\left[\alpha(A^+) + \alpha(N^+)\right] - \Delta E_i, \tag{4}$$

where the index $i = 1$, 2, or 3 refers to the final states given in (1a) and (2a), (1b) and (2b), or (1c) and (2c), respectively.[9] These potential en-

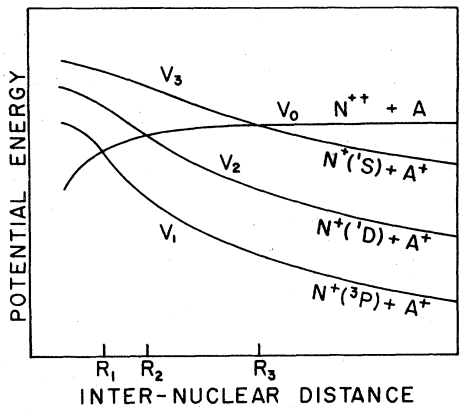

FIG. 5. Schematic illustration of the long-range potential energy curves which are involved in electron capture in the N^{2+}–He and N^{2+}–Ne collision systems.

ergy curves are illustrated in Fig. 5 and the locations of the crossing points are listed in Table I. In the LZ approximation a transition from one state to another can only occur at the point where the corresponding curves cross. The probability that the system in its initial state will remain on the diabatic curve V_0, after a single passage over the crossing point R_i, is written as

$$p_i = \exp\left\{-\frac{2\pi H_{0i}^2(R_i)}{v\,|V_0'(R_i) - V_i'(R_i)|\,\hbar}\left[1-\left(\frac{b}{R_i}\right)^2\right]^{-1/2}\right\}, \tag{5}$$

where v is the velocity of approach, b the impact parameter, H_{0i} the matrix element coupling the initial and final states, and $V_i'(R_i) = [dV_i(R)/dR]_{R=R_i}$, the slope of the curve V_i at the crossing point. A transition probability is determined by the successive application of the LZ approximation at each crossing point encountered on a path along the potential curves which leads from the initial state to some final state. The transition probabilities for the processes in (1) or (2) are

$$P(^3P) = 2p_3p_2p_1(1-p_1), \tag{6a}$$

$$P(^1D) = (1-p_2)[2p_3p_2 - P(^3P)], \tag{6b}$$

$$P(^1S) = (1-p_3)[2p_3 - P(^1D) - P(^3P)]. \tag{6c}$$

The cross sections for the corresponding processes are obtained by integration over the range of impact parameters inside the appropriate crossing point:

$$Q(L_i) = 2\pi\int_0^{R_i} P(L_i)\,b\,db; \quad L_i = {}^3P,\ {}^1D,\ \text{or}\ {}^1S. \tag{7}$$

We have computed the LZ cross sections for the processes under investigation (see Fig. 6). Initially these cross sections were calculated using the coupling matrix elements H_{0i} given by the semiempirical formula of Olson, Smith and Bauer (OSB).[8] These matrix elements were then adjusted by a multiplicative factor F_i in an attempt to obtain the best fit to the experimental data.

1. N^{2+}-He collisions

Our energy-change spectra demonstrate that the production of $N^+(^3P)$ in electron-capture collisions between N^{2+} and He [process (1a)] is far more probable than the production of excited N^+ [processes (1b) and (1c)]. Thus the total electron-capture cross sections reported by Hasted and

TABLE I. Parameters used in calculations of electron-capture cross sections in the N^{2+}–He and N^{2+}–Ne systems.

Dipole polarizability				
Atomic state	He(^1S)	He$^+$(^2S)	Ne(^1S)	Ne$^+$(^2P)
$\alpha(a_0^3)$	1.4[a]	0.28[c]	2.7[a]	1.4[c]
Atomic state	$N^+(^3P)$	$N^+(^1D)$	$N^+(^1S)$	
$\alpha(a_0^3)$	3.35[a]	3.56[b]	3.95[b]	
		N^{2+} – He		
Product state	$N^+(^3P)$	$N^+(^1D)$	$N^+(^1S)$	
ΔE_i (a.u.)	0.184	0.115	0.0356	
$R_i(a_0)$	5.4	8.7	28	
$H_{0i}^{OSB}(R_i)$ (a.u.)[d]	1.6×10^{-2}	3.6×10^{-4}	2.5×10^{-13}	
		N^{2+} – Ne		
Product state	$N^+(^3P)$	$N^+(^1D)$	$N^+(^1S)$	
ΔE_i (a.u.)	0.296	0.226	0.147	
$R_i(a_0)$	3.6	4.5	6.8	
$H_{0i}^{OSB}(R_i)$ (a.u.)[d]	6.9×10^{-2}	2.9×10^{-2}	3.3×10^{-3}	

[a]Reference 21.
[b]Reference 22.
[c]Reference 9.
[d]Reference 8.

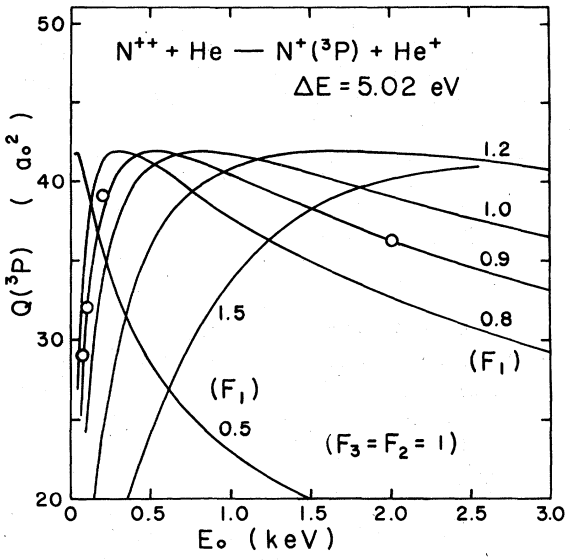

FIG. 6. Landau-Zener approximation of the cross section for charge exchange between $N^{2+}(^3P)$ and He to yield $N^+(^3P)$. The factors F_i refer to multiplicative corrections to the coupling matrix elements (Ref. 8) used in this calculation. The circles indicate the cross sections obtained in the experiments of Hasted and Smith [Ref. 7 (a)].

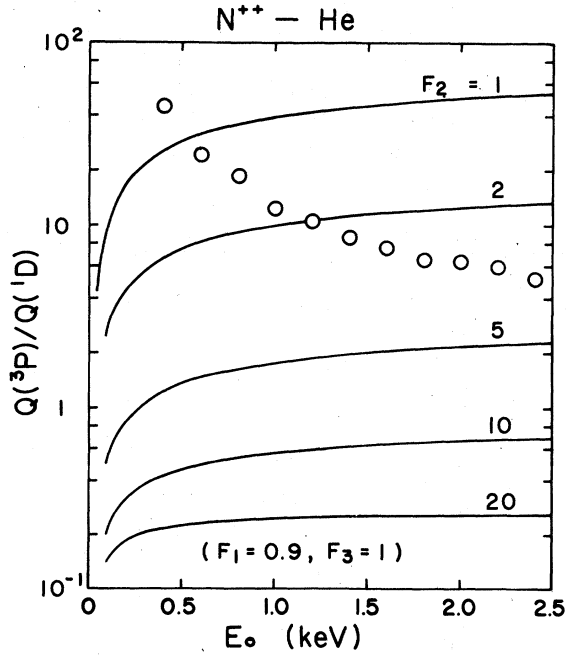

FIG. 7. Energy dependence for the ratio of electron capture cross sections $Q(^3P)/Q(^1D)$ in the N^{2+}–He system. The solid lines are the predictions of the Landau-Zener approximation for various values of the coupling matrix elements. The circles are the results of our experiments.

Smith[7(a)] can be regarded as equivalent to $Q(^3P)$, the cross section for capture into $N^+(^3P)$. We have calculated $Q(^3P)$ using the OSB coupling matrix elements, H_{0i}^{OSB}. The element $H_{0i}^{OSB}(R_i)$ has been adjusted by a factor of F_i to give agreement with the data of Hasted and Smith. Since the cross section is not sensitive to $H_{02}(R_2)$ and $H_{03}(R_3)$, which are small, these matrix elements were not varied. The statistical weight problem discussed below was ignored in these calculations. Nevertheless, the calculation with $F_1 = 0.9$ gives good agreement with experiment.

The calculation of the ratio $Q(^3P)/Q(^1D)$ is compared in Fig. 7 with our experimental data. H_{02} was varied over a wide range while H_{01} and H_{03} were set to 0.9 H_{01}^{OSB} and H_{03}^{OSB}, respectively. The value of H_{03} is not important in the calculation of $Q(^3P)/Q(^1D)$ since p_3 is a factor for both $Q(^3P)$ and $Q(^1D)$. Assuming that $H_{01}(R_1) > H_{02}(R_2)$ since $R_1 < R_2$, it was not possible to reproduce the negative energy dependence that was observed experimentally. In order to predict this negative energy dependence on the basis of the curve-crossing mechanism it is necessary to choose a value of H_{02} larger by two orders of magnitude than H_{02}^{OSB} With such a large value of H_{02}, $Q(^1D)$ becomes larger than $Q(^3P)$, contrary to the experimental results.

Hasted and his colleagues[9] have suggested that the curve V_0^*, corresponding asymptotically to $N^{2+}(^4P) + He(^1S)$, may be involved in the production of N^+. V_0^* is nearly parallel to V_0 and crosses V_1 and V_2 at $R_1^* = 2.3\,a_0$ and $R_2^* = 2.7\,a_0$, respectively. This curve could be involved via the path

$$V_0 \xrightarrow{R1} V_1 \xrightarrow{R_1^*} V_0^* \xrightarrow{R_2^*} V_2 \longrightarrow N^+(^1D) + He^+(^2S),$$

however, it should be noted that the state corresponding to V_0 is a doublet spin state while V_0^* is a quartet. V_1 has both doublet and quartet components. By the Wigner rule, V_0 couples only with the doublet component of V_1 which cannot in turn couple with V_0^*. The transition from V_0^* to V_2 is likewise forbidden. Additionally, it should be noted that transition at R_1^* would result in the production of $N^{2+}(^4P)$ which was not observed.

As was the case for the ratio $Q(^3P)/Q(^1D)$, the LZ approximation predicts that the ratio $Q(^3P)/Q(^1S)$ is an increasing function of the collision energy. Experimentally it was observed that $Q(^3P)/Q(^1S)$ decreases with increasing energy and that $Q(^1S)$, although small, is much larger than would be expected from the coupling matrix element $H_{03}^{OSB}(R_3)$ in the LZ calculation.

It is apparent that the LZ curve-crossing mechanism is not adequate to predict the relatively large transition probability between curves which

cross at large internuclear distances. It will be suggested below that the Demkov mechanism may be important in these cases.

2. N^{2+}-Ne collisions

For ratios $Q(^1S)/Q(^1D)$ and $Q(^3P)/Q(^1D)$ for the N^{2+}-Ne system were calculated for a number of different sets of correction factors (F_1, F_2, F_3). As can be seen in Figs. 8 and 9, any plausible set of coupling matrix elements give the energy dependence of these ratios that was observed in the experiments. Furthermore, when the matrix elements are all set to about 0.5 times the OSB values, the agreement between theory and experiment is about as good as can reasonably be expected from the Landau-Zener approximation.

B. Demkov mechanism

The Demkov mechanism describes a transition between two states represented by potential curves which lie close to one another but do not intersect.[12-16] The probability of a transition between two such states is largest at a critical internuclear separation R_c, where the spacing between the corresponding potential curves $V_i(R)$ and $V_j(R)$ satisfies the relation

$$2H_{ij}(R_c) = |V_i(R_c) - V_j(R_c)| . \tag{8}$$

In the approximation of Melius and Goddard (MG)[15] the probability of a transition near R_c is given by

$$p_c = 2(\operatorname{sech}\delta)\, e^{-\delta} \times \sin^2\{\tfrac{1}{4}\arctan[\sinh\lambda(R_c - b)] + \tfrac{1}{8}\pi\}, \tag{9}$$

where the characteristic parameter

$$\delta = \pi H_{ij}(R_c)/\hbar\lambda v . \tag{10}$$

The rate of decay[20] of the coupling matrix element in the transition region is specified by λ:

$$H_{ij} = \kappa e^{-\lambda R} . \tag{11}$$

As a check of the MG approximation we have applied these formula to a system treated numerically by Olson[13] and have found good agreement with Olson's results.

We have considered the possibility that a transition between curves which do not cross, as described by the Demkov mechanism, may be responsible for the behavior of the cross section $Q(^1D)$ in the N^{2+}-He collision system. The feasibility of a transition directly from V_0 to V_2 was considered first. Using the OSB formula for the coupling matrix element and assuming the form of the potential curves given by Eqs. (4) and (5), a critical region between V_0 and V_2 is predicted

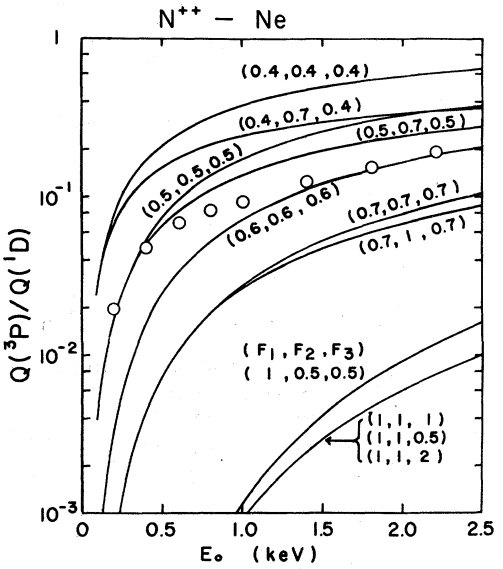

FIG. 8. Energy dependence of the ratio of electron-capture cross sections $Q(^3P)/(Q^1D)$ in the N^{2+} – Ne system. The solid lines are the predictions of the Landau-Zener approximation for various values of the coupling matrix elements. The circles are the results of our experiments.

to lie near $R_c = 3.0\,a_0$. However, the coupling matrix element at this point is so large $[H_{02}^{\mathrm{OSB}}(3.0\,a_0) = 0.32$ a.u. corresponding to $\delta \approx 11$ at $E_0 = 2$ keV] that p_c is too small to account for

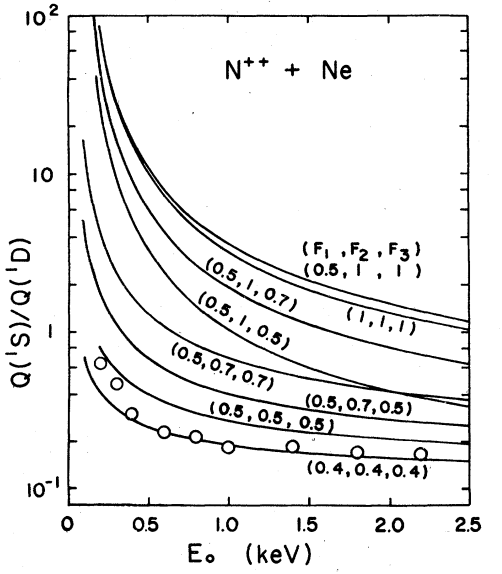

FIG. 9. Energy dependence of the ratio of electron-capture cross sections $Q(^1S)/Q(^1D)$ in the N^{2+} – Ne system. The solid lines are the predictions of the Landau-Zener approximation for various values of the coupling matrix elements. The circles are the results of our experiments.

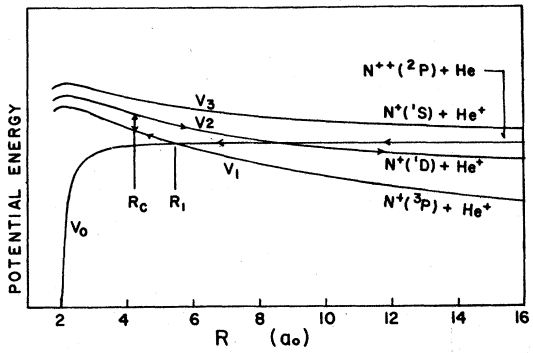

FIG. 10. Long-range portions of the potential energy curves involved in charge exchange in the N^{2+} – He system. The critical internuclear separation R_c refers to a region where the coupling between V_1 and V_2 is comparable in magnitude to the energy separation between these curves.

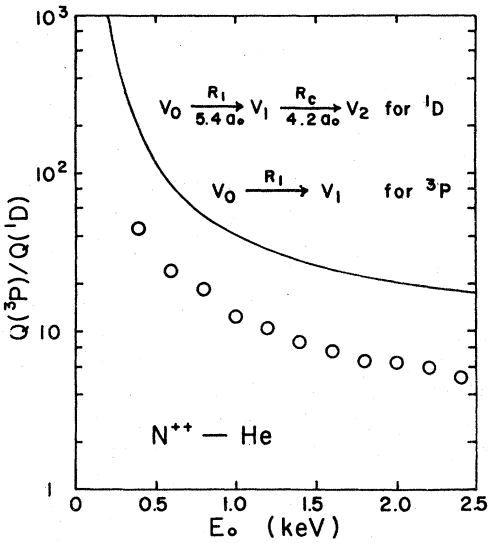

FIG. 11. Energy dependence of the ratio of electron-capture cross sections $Q(^3P)/Q(^1D)$ in the N^{2+} – He system. The solid line is a prediction based on the indicated paths for production of $N^+(^1D)$ and $N^+(^3D)$. The transition from V_0 to V_1 was calculated in the Landau-Zener approximation while the transition from V_1 to V_2 was assumed to occur by the Demkov mechanism as described by Melius and Goddard (Ref. 15). The circles are the results of our experiments.

the experimental results.

A more likely process for the production of $N^+(^1D)$ in N^{2+}-He collisions follows the path

$$V_0 \xrightarrow[4.2a_0]{R_1} V_1 \xrightarrow[4.2a_0]{R_c} V_2 ,$$

where R_c refers to the critical point between V_1 and V_2 which occurs at $R_c = 4.2\,a_0$ (Fig. 10). The total transition probability for this process is

$$P(^1D) = 2(1-p_1)p_c(1-p_c) , \qquad (12)$$

where p_1 is given by Eq. (5), p_c by Eq. (9), and the possibility of transitions at R_2 and R_3 has been ignored. The coupling matrix element at R_c is $H_{12}^{OSB}(4.2\,a_0) = 0.035$ a.u. The cross section, given by

$$Q(^1D) = 2\pi \int_0^\infty P(^1D)\, b\, db , \qquad (13)$$

has been calculated and compared with $Q(^3P)$ calculated in the LZ approximation [Eq. (11)]. A comparison between the calculated and experimentally observed energy dependence of the ratio $Q(^1D)/Q(^3P)$ is presented in Fig. 11. The energy dependence predicted by this theory is in good agreement with the experiment although the predicted magnitude of $Q(^1D)$ differs from the observed value by about a factor of 4.

The Demkov mechanism may be invoked in a similar manner to give a reasonable description of the production of $N^+(^1S)$ in N^{2+}-He collisions. As before, direct coupling between V_0 and V_3 is unimportant ($R_c = 2.0\,a_0$, $\delta \approx 18$ at $E_0 = 2$ keV). However for processes such as

$$V_0 \xrightarrow{R_1} V_1 \xrightarrow[3.4a_0]{R_c} V_3$$

or

$$V_0 \xrightarrow[4.2a_0]{R_1} V_1 \xrightarrow[4.1a_0]{R_c} V_2 \xrightarrow{R_c} V_3$$

the critical transition regions occur at intermediate distances where δ is approximately unity and relatively large transition probabilities are predicted for the Demkov processes.

C. Statistical weights

The initial and final states of the collision systems have heretofore each been represented by a single potential curve. This is only accurate at large internuclear distances. At small distances each curve may be split into several components each corresponding to one of the molecular states which is correlated with the separated atomic states. This splitting is illustrated schematically in Fig. 12 for the N^{2+}-He system. To predict the transition probabilities in such a system it is necessary to consider the nature of the coupling of each component of the initial state with each final-state component. We will assume, for example, that the most rigorous possible selection rules hold:

$$+ \not\leftrightarrow -, \quad \Delta S = 0, \quad \Delta\Lambda = 0$$

in which case $\Sigma^+ - \Sigma^-$ coupling and $\Sigma - \Pi$ rotational coupling are prohibited. Then for the N^{2+}-He system, transitions can only occur at the points

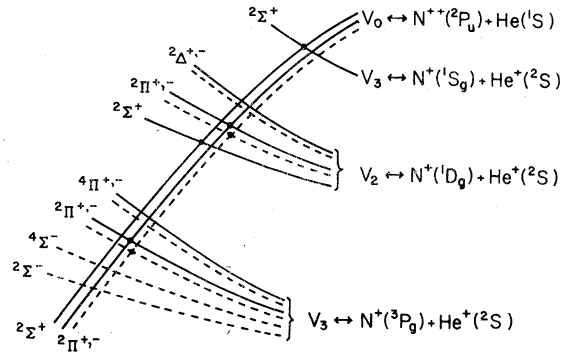

FIG. 12. Schematic illustration of the potential curves for the N^{2+} – He system showing the molecular components which correlate with the initial and each final state. Points indicate the intersections where transitions can occur if all symmetry selection rules apply.

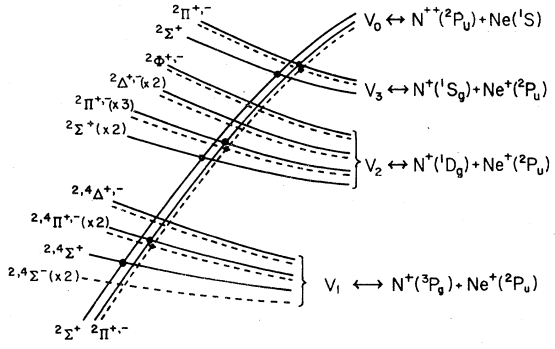

FIG. 13. Schematic illustration of the potential curves for the N^{2+} – Ne system showing the molecular components which correlate with the initial and each final state. The degeneracy of each component is given in parenthesis. Points indicate the intersections where transitions can occur if all symmetry selection rules apply.

indicated in Fig. 12. In this event the probabilities for transitions from the $^2\Sigma^+$ component of the initial state to the various final states are

$$P_\Sigma(^3P) = 0\,, \tag{14a}$$

$$P_\Sigma(^1D) = 2p_3^\Sigma p_2^\Sigma(1-p_2^\Sigma)\,, \tag{14b}$$

$$P_\Sigma(^1S) = 2p_3^\Sigma(1-p_3^\Sigma)[1-p_2^\Sigma(1-p_2^\Sigma)]\,, \tag{14c}$$

where p_i is the LZ transition probability for a pair of Σ curves crossing at R_i. Similarly for the $^2\Pi^+$ or $^2\Pi^-$ components of the initial state

$$P_\Pi(^3P) = 2p_2^\Pi p_1^\Pi(1-p_1^\Pi)\,, \tag{15a}$$

$$P_\Pi(^1D) = 2p_2^\Pi(1-p_2^\Pi)[1-p_1^\Pi(1-p_1^\Pi)]\,, \tag{15b}$$

$$P_\Pi(^1S) = 0\,. \tag{15c}$$

The overall transition probability is given by

$$P(L_i) = \tfrac{1}{3}[(P_\Sigma(L_i)+2P_\Pi(L_i)]\,;\quad L_i = {}^3P, {}^1P, \text{ or } {}^1S\,. \tag{16}$$

If the coupling matrix elements between Σ states and between Π states at R_2 are assumed to be equal then

$$P(^1D) = 2p_2(1-p_2)[1-\tfrac{2}{3}p_1(1-p_1)] \tag{17}$$

when p_3^Σ is taken to be unity since the crossing point R_3 is so distant.

The N^{2+}-Ne system (Fig. 13) is more complicated since the product rare-gas ion is in a ^2P state rather than a ^2S state. This means that many of the final-state components are multiply degenerate. The $^2\Pi$ components of the V_1 state are each doubly degenerate, the $^2\Sigma^+$ component of the V_2 state is doubly degenerate, and the $^2\Pi$ components of the V_2 state are each triply degenerate. Furthermore, the V_3 state acquires a $^2\Pi^+$ and $^2\Pi^-$ component. The coupling between degenerate components must be considered since even if they do not couple directly, they are coupled through the component of V_0 which has the same symmetry. We will present as an example a simple model for dealing with crossings of degenerate states.

Consider the crossings of Π components near R_2 in the N^{2+}-Ne system. The state which corresponds to the $^2\Pi^+$ component of V_2 is composed of three degenerate $^2\Pi^+$ states:

$$\phi_2^\Pi = \frac{1}{\sqrt{3}}(\phi_{2a}^\Pi + \phi_{2b}^\Pi + \phi_{2c}^\Pi) \tag{18}$$

Assume that (i) the degenerate states do not couple with one another so that

$$\langle\phi_{2k}^\Pi|H^{el}|\phi_{2l}^\Pi\rangle = \delta_{kl}V_2(R);\quad k,l = a,b,c \tag{19}$$

where δ_{kl} is the Kronecker delta function, and (ii) the coupling between the $^2\Pi^+$ state of V_0 and each of the degenerate $^2\Pi^+$ components of V_2 is the same:

$$\langle\phi_0^\Pi|H^{el}|\phi_{2k}^\Pi\rangle = H_{02}^\Pi\,. \tag{20}$$

Then the matrix elements of the electronic Hamiltonian between the Π components of V_0 and V_2 are

$$\langle\phi_0^\Pi|H^{el}|\phi_0^\Pi\rangle = V_0(R)\,, \tag{21}$$

$$\langle\phi_2^\Pi|H^{el}|\phi_2^\Pi\rangle = V_2(R)\,, \tag{22}$$

$$\langle\phi_0^\Pi|H^{el}|\phi_2^\Pi\rangle = \sqrt{3}\,H_{02}^\Pi\,. \tag{23}$$

Similarly the coupling between individual Π components of V_0 and V_1 and between V_0 and V_3 are given by $\sqrt{2}H_{01}^\Pi$ and H_{03}^Π, respectively. Furthermore, on the basis of this simple model it can be seen that the matrix elements for the individual $\Sigma-\Sigma$ couplings are H_{01}^Σ, $\sqrt{2}H_{02}^\Sigma$, and H_{03}^Σ.

The transition probabilities between $^2\Sigma^*$, $^2\Pi^+$, and $^2\Pi^-$ components are each written in the forms given by Eqs. (6) and overall transition probabilities are given by the summation of Eq. (16).

Then if $\sqrt{2}\,H^{\Pi}_{01}=H^{\Sigma}_{01}\equiv H_{01}$, $\sqrt{3}\,H^{\Pi}_{02}=\sqrt{2}\,H^{\Sigma}_{02}\equiv H_{02}$, and $H^{\Pi}_{03}=H^{\Sigma}_{03}\equiv H_{03}$, a crossing at R_i is considered as a single crossing with coupling matrix element H_{0i} and a statistical weight of unity.

The simple models presented above for dealing with the multiplicity of each state of a collision system are probably appropriate to the LZ approximation which must be regarded as semiquantitative at best. A more rigorous consideration of the nature of the coupling between states of different symmetry would be required if a more precise theoretical description were to be applied. In any case, our conclusions in Secs. IV (A) and B above concerning the energy dependence of ratios of cross sections are not much affected by consideration of degeneracy and statistical weight problems.

V. CONCLUSION

Our results demonstrate that the nature of the curve-crossing phenomenon can be classified according to the internuclear distance at which a transition occurs. Crossings which occur at distances $R \gtrsim 8\,a_0$ are not likely to result in a transition from one state to another. This is the diabatic or atomic region where the coupling between states is weak and the collision system is best described as two independent atomic systems. Crossings at distances $R \lesssim 3.5\,a_0$ are also not likely to result in a net transition from one state to another. In this region the coupling matrix element is large and the system is best described by adiabatic potential curves which do not cross. A transition is most likely to occur between curves which cross in the region intermediate between the diabatic and adiabatic regions. Curve crossings at these intermediate distances are responsible for the large cross sections observed for processes (2a) and (3b). The extent of coupling between atomic states to give molecular or adiabatic states depends upon the velocity of approach of the collision partners. As the collision velocity increases, the transition region moves toward smaller internuclear distances. Thus the probability of a transition at the crossing at $3.6\,a_0$ in the N^{2+}-Ne system [process 3(a)] increases with increasing collision velocity. When a pair of curves pass close to one another but do not cross in the intermediate region then it appears that the possibility of a transition via a process of the type described by the Demkov mechanism must be considered.

ACKNOWLEDGMENTS

This work was supported by NSF Grant No. CHE-7708523 and by a grant from the Computer Science Center of the University of Maryland. One of the authors (Y. S.) acknowledges a fellowship from the Yoshida Foundation. We are grateful to Professor M. H. Alexander for several helpful discussions.

*On leave from Tohoku University, Sendai, Japan
[1]D. R. Bates and B. L. Moiseiwitsch, Proc. Phys. Soc. A 67, 805 (1954); A. Dalgarno, Proc. Phys Soc. A 67, 1010 (1954). D. R. Bates and J. T. Lewis, Proc. Phys. Soc. A 68, 173 (1955). D. R. Bates and J. M. Boyd, Proc. Phys. Soc. A 69, 910 (1956).
[2]T. J. M. Boyd and B. L. Moiseiwitsch, Proc. Phys. Soc. A 70, 809 (1957).
[3]L. D. Landau, J. Phys. (Moscow) 2, 46 (1932).
[4]C. Zener, Proc. Roy. Soc. A 137, 696 (1932).
[5]E. C. G. Stueckelberg, Helv. Phys. Acta. 5, 370 (1932).
[6]See, for example, D. R. Bates, Proc. R. Soc. Lond. A 259, 22 (1960); J. S. Cohen, S. A. Evans, and N. F. Lane, Phys. Rev. A 4, 2235 (1971); 4, 2248 (1971); J. B. Delos and W. R. Thorson, Phys. Rev. A 6, 728 (1972).
[7](a) J. B. Hasted and R. A. Smith, Proc. R. Soc. Lond. A 235, 349 354 (1956); (b) J. B. Hasted and A. Y. J. Chong, Proc. R. Soc. Lond. 80, 441 (1962); (c) J. B. Hasted and M. Hussain, Proc. Phys. Soc. Lond. 83, 911 (1964).
[8]R. E. Olson, F. T. Smith, and E. Bauer, Appl. Optics 10, 1848 (1971).
[9]J. B. Hasted, S. M. Igbal, and M. M. Yousaf, J. Phys. B 4, 343 (1971).
[10]Y. Y. Makhdis, K. Birkinshaw, and J. B. Hasted, J. Phys. 9, 111 (1976).
[11]Y. H. Chen, R. E. Johnson, R. R. Humphris, M. W. Siegel, and J. W. Boring, J. Phys. B 8, 1527 (1975).
[12]Y. N Demkov, Sov. Phys. JETP 18, 138 (1964).
[13]R. E. Olson, Phys. Rev. A 6, 1822 (1972).
[14]R. E. Olson and F. T. Smith, Phys. Rev. A 7, 1529 (1973).
[15]C. F. Melius and W. A. Goddard III, Phys. Rev. A 10, 1541 (1974).
[16]M Barat, J. C. Brenot, D. Dhuicq, J. Pommier, V. Sidis, R. E. Olson, E. J. Shipsey, and J. C. Brownes, J. Phys. B 9, 269 (1976).
[17]J. H. Moore, Jr., J. Chem. Phys. 55, 2760 (1971).
[18]E. Wigner, Nachr. Akad. Wiss. Goett. Math. Phys. Kl. *IIa*, 375 (1927); J. H. Moore, Phys. Rev. A 8, 2359 (1973); 10, 724 (1974).
[19]In a preliminary study (to be published) on the charge transfer from Ar to N^{2+}, the $N^{+}(^3D)$ state was found to be the major product.
[20]Following Olson and Smith (Ref. 14), the decay factor for a reaction $A^{+}+B\rightarrow A+B^{+}$ is estimated by $\lambda=0.61(\sqrt{I_A}+\sqrt{I_B})$ where I_A and I_B are the ionization potentials of A and B, respectively.
[21]J. Thorhallson, C. Fisk, and S. Fraga, Theor. Chim. Acta 10, 390 (1968).
[22]S. Fraga and K. M. S. Saxena, At. Data 4, 225 (1972).